

DDO 187: do dwarf galaxies have extended, old halos?¹

Antonio Aparicio

Instituto de Astrofísica de Canarias, E38200 - La Laguna, Tenerife, Canary Islands, Spain

Nikolay Tikhonov and Igor Karachentsev

Special Astrophysical Observatory, Stavropol, Russia

ABSTRACT

If dwarf galaxies are primeval objects in the Universe, as hierarchical galaxy formation scenarios predict, they should show traces of their old stellar populations, perhaps distributed in extended, differentiated structures. The working hypothesis that such a structure could exist is tested for the case of DDO 187, a field dIrr galaxy showing a high gas fraction and low metallicity. For this purpose, the structure, star formation history (SFH) and other properties of the galaxy are analyzed using the spatial distribution of stars, the color–magnitude diagrams (CMDs) of about 1500 resolved stars and the fluxes of H II regions, together with data about the gas distribution.

From the I magnitude of the tip of the red giant branch (I_{TRGB}), the distance of DDO 187 to the Milky Way is estimated to be 2.5 ± 0.2 Mpc. The distance to several neighbor galaxies and groups has been computed, showing that DDO 187 is probably an isolated, field galaxy.

The distance of DDO 187 to the Milky Way is almost three times smaller than that obtained from Cepheid light-curves. Considering that this is the third case in which such a large disagreement is detected, it seems clear that Cepheid distance estimates based on a few stars, as usually happens in dwarf galaxies, must be accepted with caution.

The star formation history of DDO 187 has been analyzed. The central region of DDO 187 shows an overall time decreasing star formation rate with a strong burst in its central region which happened between 20 and 100 Myrs ago and a present-day star formation activity three times smaller than the maximum one. Besides this, a spatially extended stellar component has been found that has no young stars and exceeds the size of the gas component.

¹Based on observations made with the 2.5 m Nordic Optical Telescope operated on the island of La Palma by NOT S.A. in the Spanish Observatorio del Roque de Los Muchachos of the Instituto de Astrofísica de Canarias.

In short, several results suggest that DDO 187 has a two-component halo/disk-like structure: (i) differentiated morphologies for the inner (flat) and outer (spheroidal) stellar components; (ii) a gas component less extended than the outer stellar component, and (iii) an outer component lacking young stars, which are abundant in the inner component. The working hypothesis that a real halo/disk structure could be present is discussed. The conclusion is reached that the two-component hypothesis is not unrealistic, but nothing can be definitely stated until more detailed data, ideally including kinematics, are available.

Subject headings: galaxies: distances and redshifts — galaxies: dwarf — galaxies: fundamental parameters — galaxies: halos — galaxies: individual (DDO 187) — galaxies: irregulars — galaxies: stellar content — galaxies: structure

1. Introduction

In hierarchical scenarios of galaxy formation (White & Rees 1978), dwarfs would be the first galaxies to be formed, from small-amplitude density fluctuations and would later on merge to form larger galaxies and structures. The fact that the gas-poor, dEs are usually found in denser parts of the Universe than the gas-rich dIrrs may indicate that both have the same origin, the former being in a more evolved evolutionary stage and in the process of being soon incorporated into bigger neighboring galaxies. If this were the case, isolated dIrrs like DDO 187 should still have the traces of their formation process and early evolution and, eventually, a similar underlying structure to that of the less distorted dEs. It is hence of major relevance to study the structure, kinematics and spatial distribution of stellar populations, including the oldest ones, of these small, gas rich galaxies, checking in particular whether they have old/young subsystems similar to the halo/disk ones of spirals or any other structures that would trace their formation scenario. The main purpose of this paper is to test the hypothesis of the existence of a two-component, halo/disk structure in the field dIrr galaxy DDO 187.

DDO 187 (UGC 9128) is a resolved, gas-rich dwarf galaxy first cataloged by van den Bergh (1959). It shows a morphology typical of dIrr galaxies, with the bluest stellar population lying on one-half of its body, and has been subject of several works directed toward the study of its distance, stellar content, neutral gas, and chemical abundances. Aparicio, Moles, & García-Pelayo (1988) showed a color–magnitude diagram (CMD) and roughly estimated the distance to the galaxy to be 4.4 ± 1.0 Mpc, based on the magnitude

of the brightest stars. Skillman, Kennicutt, & Hodge (1989) found a very low oxygen abundance of $12 + \log \text{O}/\text{H} = 7.36$. Recently, van Zee, Haynes, & Salzer (1997a) have obtained $12 + \log \text{O}/\text{H} = 7.75$ and 7.73 for two H II regions in the galaxy. Lo, Sargent, & Young (1993) determined its heliocentric H I velocity (153 km s^{-1}) and using a distance of 4 Mpc, obtained its H I and total virial masses to be $M_{\text{H}} = 5 \times 10^7 M_{\odot}$ and $M_{\text{VT}} = 9.8 \times 10^7 M_{\odot}$. Van Zee, *et al.* (1997b), assuming a distance of 3.4 Mpc, obtained $M_{\text{H}} = 3.5 \times 10^7 M_{\odot}$. Using surface photometry, Patterson & Thuan (1996) derived an exponential scale length of 0.25 kpc, for a distance of 4.4 Mpc. Recently Hoessel, Saha, & Danielson (1998) presented the results of their time-extended research of variable stars in DDO 187. They find 12 variable stars, and identify two of them as very likely Cepheids and three more as possible Cepheids. Using their periods and luminosities, they derive a distance of 7.0 ± 1.2 Mpc for DDO 187.

We present new ground-based V , I , and H_{α} photometry of DDO 187 and analyze the properties of this galaxy. The paper is organized as follows. Observations are described in Section 2. The CMD of the resolved stars is presented in Section 3. Our photometry reach the tip of the red giant branch (TRGB), allowing an independent determination of the distance, which does not agree with the Cepheid-based one. This is discussed in Section 4. The ionized distribution of H and the properties that can be inferred for the ionizing stars are discussed in Section 5. Section 6 is devoted to the study of the structure, star formation history (SFH), and spatial distribution of stellar populations, discussing, in particular, the hypothesis that DDO 187 had a two-components (halo/disk-like) structure. In Sec. 7, several global properties of the galaxy are given. Finally, Sec. 8 summarizes the main results of the paper.

2. Observations and data reduction

Images of DDO 187 were obtained in the V and I Johnson–Cousins filters and in a narrow-band H_{α} filter with the NOT (2.5 m) at Roque de los Muchachos Observatory on the island of La Palma (Canary Islands, Spain). The HiRAC camera was used with a 2048×2048 Loral CCD binned to 2×2 . After binning it provides a scale of $0.22''/\text{pix}$ and a total field of $3.75 \times 3.75 \text{ arcmin}^2$. Total integration times were 3600 s in V , 3000 s in I , and 1200 s in H_{α} . A 400 s exposure was also taken with an H_{α} -continuum filter. Moreover, integrations of 1200 s in V and 1000 s in I were made of a nearby field to correct the foreground contamination of the broad-band images. Observations of DDO 187 were taken with seeing always in the range $0''.7 - 0''.9$. Table 1 gives the journal of observations. Figure 1 shows one of the I band images of DDO 187. A beautiful picture of the galaxy can be

seen in Hoessel *et al.* (1998).

Bias and flat-field corrections were done with IRAF. Then, DAOPHOT and ALLSTAR (Stetson 1994) were used to obtain the instrumental photometry of the stars. Eighteen standard stars from the list of Landolt (1992) were measured during the observing run to calculate the atmospheric extinctions for each night and the equations transforming into the Johnson–Cousins standard photometric system. A total of about 180 measures in both the V and I bands of these standards were used. The transformation equations are:

$$(V - v) = 25.205 - 0.106(V - I); \quad \sigma = 0.005 \quad (1)$$

$$(I - i) = 24.498 + 0.011(V - I); \quad \sigma = 0.004 \quad (2)$$

where capital letters stand for Johnson–Cousins magnitudes and lower-case letters refer to instrumental magnitudes corrected for atmospheric extinction. The σ values are the dispersions of the fits at the centers of mass of the point distributions; hence they are the minimum internal zero-point errors. Dispersions of the extinctions for each night vary from $\sigma = 0.009$ to $\sigma = 0.019$ and dispersions of the aperture corrections are of the order of 0.04. Putting all these values together, the total zero-point error of our photometry can be estimated to be about 0.05 for both bands.

One standard star from Oke (1990) was observed three times to calibrate the H_α images. The dispersion of the measures was better than 0.01 magnitudes.

DAOPHOT and ALLSTAR provide with PSF model to star profile fitting errors. In general, they do not reproduce the external errors of the photometry, coming mainly from stellar crowding and blending (see Aparicio, & Gallart 1995 and Gallart, Aparicio, & Vílchez 1996a), but they provide with an indication of the internal accuracy of the photometry. In this sense, our average ALLSTAR errors are 0.01, 0.04 and 0.16 for $I = 20$, 22 and 24 respectively and for $V = 21.2$, 23.3 and 25.4, respectively.

3. The color–magnitude diagram

The CMD of DDO 187 is shown in Figure 2. It is typical of a resolved galaxy with recent star formation (compare, for example, with the richer CMD of NGC 6822 by Gallart *et al.* 1996a). A well populated structure is visible in the region $I \geq 23$, $1.0 \leq (V - I) \leq 1.8$. It corresponds to the *red-tangle* (see Aparicio & Gallart 1994; Aparicio *et al.* 1996). It is formed by low-mass stars in the RGB and AGB phases and it is hence the trace of an intermediate-age to old stellar population. A well populated blue-plume is also visible at

$I \geq 21.5$, $(V - I) \leq 0.8$. Formed by intermediate to massive stars in the MS and/or the core He-burning blue-loop phases, it is the trace of significant recent star formation, in good agreement with the presence of H II regions in the galaxy. At least some of the red stars in the region $20.5 \leq I \leq 23$, $(V - I) \geq 1.6$ are likely AGB stars forming a *red-tail* structure of the kind discussed by Aparicio & Gallart (1994).

Figure 3 shows the CMD of a companion field, close to DDO 187 but far enough to guarantee that it contains no stars of the galaxy. The distribution of stars in this diagram indicates that most stars brighter than $I \sim 21$ and some of the fainter in the CMD of Fig. 2 are foreground stars belonging to the Milky Way. The CMD of Fig. 3 will be used to correct for foreground contamination the star counts in DDO 187 used in Section 6.

In summary, the CMD of DDO 187 indicates that it has had an extended SFH, as evidenced by the presence of young blue stars and a red-tangle of intermediate-age and/or old stars. A quantitative estimate of the SFH is given in Section 6.2.

4. The distance of DDO 187

4.1. The distance from the TRGB

Hoessel *et al.* (1998) made a wide time coverage survey of variable stars in DDO 187. They identified two stars in the galaxy as very likely Cepheids and three more as possible Cepheids. Using them, they determine a distance of 7.0 ± 1.2 Mpc. This distance implies that the TRGB of DDO 187 should be fainter than $I \sim 25$, and hence difficult to reach by usual ground-based telescopes.

However, this seems not to be the case in the light of the CMD shown in Figure 2. An independent estimate of the distance to DDO 187 can be made using the magnitude of the TRGB and the relationships of Lee, Freedman, & Madore (1993). We have determined the magnitude of the TRGB from the CMD of Fig. 2, applying a Sobel filter to the luminosity function (LF) of stars with colors in the interval $1.3 \leq (V - I) \leq 1.7$, and obtained $I_{\text{TRGB}} = 22.95 \pm 0.17$. The error has been estimated from the width of the peak produced by the Sobel filter around the TRGB. Several binning sizes and initial values for the LF were used, the former result being the average of all them.

Crowding, blending and other observational effects modify the measured star magnitudes in the sense that, in average, they appear brighter than they are (see a discussion of this in Aparicio, & Gallart 1995 and Gallart *et al.* 1996a). This would eventually affect the magnitude of the TRGB. To check this effect and for the analysis

of the stellar populations presented in Section 6, we have performed crowding tests using artificial stars in the way described by Stetson (1994). We have added 1190 artificial stars to our images with initial magnitude and color $I = 23.0$, $(V - I) = 1.5$, roughly corresponding to the position of the TRGB. 90% of them were recovered, their average magnitude and color being $I = 23.01 \pm 0.19$ and $(V - I) = 1.48 \pm 0.14$, showing that shifts produced by observational effects are negligible at the position of the TRGB.

The extinction towards DDO 187 can be estimated to be $E(B - V) = 0.005$ (Burstein & Heiles 1982). This can be neglected and hence the former value for $I_{\text{TRGB}} = 22.95 \pm 0.17$ can be assumed to be free of extinction and observational effects.

To apply the relationships of Lee *et al.* (1993), the metallicity of the stars and the bolometric correction (BC) at the TRGB are necessary. Both can be estimated from the color indices of RGB stars. $(V - I)_{\text{TRGB}} = 1.53 \pm 0.03$ and $(V - I)_{-3.5} = 1.45 \pm 0.04$ have been obtained as the median of the color indices of stars with $22.95 \leq I \leq 23.05$ and $23.4 \leq I \leq 23.5$ respectively and having colors in the interval $1.0 \leq (V - I) \leq 2.0$. Some 35 stars have been used in each case and the quoted errors have been simply obtained as $\sigma(n - 1)^{-1/2}$ for each sample. From $(V - I)_{-3.5}$, an average metallicity of $[\text{Fe}/\text{H}] = -1.36 \pm 0.11$ is found using the calibration by Lee *et al.* (1993). This Fe abundance corresponds to $Z = 0.0008 \pm 0.0002$, which is similar to the values obtained from the oxygen abundance of the H II regions by Skillman *et al.* (1989) and by van Zee *et al.* (1997a) ($Z = 0.0006$ and $Z = 0.001$, respectively).

These values can finally be introduced in the relationships of Lee *et al.* (1993) to obtain the absolute magnitude of the TRGB, $M_{I,\text{TRGB}} = -4.06$, and hence a distance modulus of $(m - M)_0 = 27.0 \pm 0.2$, which corresponds to a distance to the Milky Way of $d_{\text{MW}} = 2.5 \pm 0.2$ Mpc.

4.2. The distance of DDO 187 to the closest galaxies and groups

To check whether DDO 187 can be considered a field galaxy, its distance to other nearby galaxies has been computed. The selected galaxies are GR 8, DDO 187, Andromeda, M81, M94 and M101, as well as the barycenter of the Local Group. The first two galaxies are apparently the closest dwarfs to DDO 187. The other ones are the dominant members of the closest groups. The distances to the Milky Way adopted for each one are: GR 8, 2.2 Mpc (Dohm-Palmer *et al.* 1998); DDO 190, 2.9 Mpc (Aparicio *et al.* 1999); Andromeda, 0.77 Mpc (Freedman & Madore 1990); M 81, 3.6 Mpc (Freedman *et al.* 1994); M 94, 4.7 Mpc (Mulder & van Driel 1993, adopting $H_0 = 70 \text{ kms}^{-1}\text{Mpc}^{-1}$) and M 101, 7.0 Mpc

(Stetson *et al.* 1998). The position of the barycenter of the Local Group has been calculated neglecting the masses of all the galaxies in the LG except Andromeda and the Milky Way, assuming that the mass of the Milky Way is 0.7 times that of Andromeda (Peebles 1989) and adopting a value of 0.77 Mpc for the Milky Way–Andromeda distance (Freedman & Madore 1990).

In this way, the resulting distances of DDO 187 to each galaxy are: 0.85 Mpc to GR 8; 1.06 Mpc to DDO 190; 2.9 Mpc to Andromeda; 3.2 Mpc to M 81; 2.6 Mpc to M 94; 5.2 Mpc to M101 and 2.7 Mpc to the barycenter of the Local Group. Hence DDO 187 is likely a field galaxy lying between the Local, M81 and M94 groups, the closest galaxy being the dIrr GR 8. All the distances are summarized in Table 2.

4.3. The Cepheid distance problem: comparison of Cepheid and TRGB distances

The large disagreement between the Cepheid and TRGB distances merits some comment. While the Cepheid P–L relationship is the best distance indicator for nearby galaxies, its reliability has been recently questioned by several authors (Aparicio 1994; Saha *et al.* 1996; Tolstoy *et al.* 1998). The problem arises from the fact that, for several dwarf galaxies (namely, Pegasus, Leo A and, now, DDO 187), a large disagreement has been detected between Cepheid based distances and TRGB or red-clump (RC) based distances. Table 3 summarizes the distances found with each method for the three galaxies. Column 1 gives the galaxy name; columns 2 to 4 list the Cepheid distance, the number of Cepheids used to determine it and the reference; columns 5 to 7 give the CMD-based distance, the feature (TRGB or RC) used to estimate it and the reference. In all cases, Cepheid distances were based on just a few stars showing light curves resembling those of bona-fide Cepheids. However, latter accurate two-color photometry (Aparicio 1994; Tolstoy *et al.* 1998) demonstrated that the colors of these stars could in no way be reconciled with those of Cepheid stars, which is also stressed by Saha *et al.* (1996).

In the case of DDO 187, Hoessel *et al.* (1998) identified only two stars as very likely long-period Cepheids and three more, with lower quality photometry, as possible Cepheids. They used a control CMD for these stars but perhaps it was not deep enough for the purpose. Figure 4 shows our CMD with the Cepheid candidates of Hoessel *et al.* (1998) marked with filled dots. From their location in the diagram, these stars are likely AGB stars and could well be some kind of long-period variables (for further discussion on the presence of long-period variables in DDO 187 see Hoessel *et al.* 1998).

Considering that DDO 187 is the third case in which a large distance disagreement has been found, it seems clear that Cepheid distance estimates based on a few stars, as usually happens for dwarf galaxies, must be accepted with caution. Possibly, only galaxies with a large young star population, like spirals or dwarfs in a phase immediately following a strong star formation burst, are adequate for a confident use of Cepheid stars as distance indicators, since only in these galaxies a significant population of Cepheids is expected. The analysis should ever include checking colors in a reliable CMD and a good phase coverage in order to avoid aliased periods (see also Saha *et al.* 1996 on the distance of the postburst dIrr IC 10).

In the following we will use $d_{\text{MW}} = 2.5 \pm 0.2$ Mpc for the discussion of the properties of DDO 187.

5. Ionized gas

Figure 5 shows the H_α image of DDO 187, after subtraction of the continuum. We have identified 10 H II regions of different morphology and compactness. A summary of the results is given in Table 4. Column 1 gives the identification number as shown in Fig. 5, followed by a bracketed c or d indicating whether the H II region is compact or diffuse, respectively. Column 2 lists an estimate of the size. For regions 1 to 7, the sizes are the full width at half of maximum, while for the diffuse regions 8 to 10, the sizes are the square root of the total area used to calculate the flux. Column 3 gives the flux received from each region in $\text{erg s}^{-1} \text{cm}^{-2}$. Column 4 gives the corresponding H_α luminosities in erg s^{-1} calculated for a distance of 2.5 Mpc. Column 5 lists the number of ionizing photons per second required to produce those luminosities, calculated following Kennicutt (1988). Column 6 gives the masses required for single MS stars to produce such amounts of ionizing photons (they have not been calculated for the diffuse regions). To calculate these masses, the relation given in Fig. 6 has been used. It has been plotted from calculations made using the models of Panagia (1973) and the Padua stellar evolutionary library (Bertelli *et al.* 1994). It must be kept in mind that, at the distance of DDO 187, $1''$ corresponds to 12 pc, so the assumption that the H II regions are ionized by single stars may well be an oversimplification, even for the compact ones.

The total H_α flux, luminosity and number of ionizing photons are given in the last line of Table 4 including also the very diffuse emission, not comprised in the regions 1 to 10 listed in the table. N_L can be used to estimate the current SFR. It is given by

$$N_L = \int_{m_k}^{m_s} \int_0^{\tau(m)} \phi(m) \psi_n(t) n_L(m) dm dt, \quad (3)$$

where time increases from the present to the past, the present time being 0, $\phi(m)$ is the IMF, $\psi_n(t)$ is the SFR in units of number of stars per year and $\tau(m)$ is the MS life-time of a star of mass m and $n_L(m)$ is the number of Lyman photons emitted per second by a MS star of mass m . While we are interested in stars more massive than some $10 M_\odot$ (see Table 2) we need to consider only the interval of time 0 to $\tau(10)$. If, for simplicity, we assume that the SFR is constant over this interval, then

$$N_L = \psi_n(0) \int_{m_k}^{m_s} \phi(m) n_L(m) \tau(m) dm, \quad (4)$$

where $\psi_n(0)$ is the constant current value of the SFR in yr^{-1} . Using data for stars of metallicity $Z = 0.0004$ from the stellar evolutionary library of Padua (see Bertelli *et al.* 1994) the MS life-time (in years) can be approximated analytically by

$$\tau(m) = 2.24 \times 10^8 m^{-1}. \quad (5)$$

Moreover, for masses in the interval $12M_\odot \leq m \leq 40M_\odot$, $n_L(m)$ can be approximated analytically by

$$n_L(m) = 10^{48} (1.352 - 0.288 m + 0.015 m^2). \quad (6)$$

Introducing the IMF of Kroupa, Tout, & Gilmore (1993), equation (4) becomes

$$N_L = S \times \psi_n(0), \quad (7)$$

with $S = 0.91 \times 10^{52}$, 1.29×10^{52} , or 1.92×10^{52} for $m_s = 25M_\odot$, $30M_\odot$ and $40M_\odot$, respectively. The result is almost insensitive to the value of m_k , which has been fixed to $m_k = 12M_\odot$. Using the total value of N_L given in Table 4, the current SFR can be adopted to be $\psi_n(0) = (3.44 \pm 1.22) \times 10^{-3} \text{yr}^{-1}$. It is better to give the SFR in units of mass. From integration of the Kroupa *et al.* (1993) IMF from $0.1 M_\odot$ to ∞ the average mass of the stars results $0.51 M_\odot$ and so the SFR becomes $\psi(0) = (1.75 \pm 0.62) \times 10^{-3} M_\odot \text{yr}^{-1}$. This can be assumed to be the SFR in DDO 187 averaged for the last ~ 20 Myr. Different IMFs would produce different results for the SFR. For comparison, using a Salpeter IMF ($\phi(m) = Am^{-2.35}$) with lower mass limit $m_i = 0.1 M_\odot$, would produce a SFR 10% smaller than the former value.

6. Morphology, star formation history and structure of DDO 187: testing the halo/disk hypothesis

Evident galactocentric gradients in the young stellar population have recently been found in several dIrrs: WLM (Minniti & Zijlstra 1996); Antlia (Aparicio *et al.* 1997c);

Phoenix (Martínez-Delgado, Gallart, & Aparicio 1999); NGC 3109 (Minniti, Zijlstra, & Alonso 1999). All these galaxies have undergone recent star formation episodes in their centers, but lack young stars in outer regions. However the conclusion cannot be drawn from this fact alone that they have two differentiated structures, the outer being an old subsystem tracing out the formation and early evolution of the galaxy. This result would not be surprising, but sufficiently accurate age distributions and structural and kinematical information are needed before confidently accepting it.

Interesting steps towards establishing the primeval nature of the extended structures are supplied by Minniti, & Zijlstra (1997) who provide with clues compatible with an old age of the extended population in WLM (although the presence of an intermediate-age component can not be, in our opinion, excluded) and include a morphological analysis concluding that flattening is smaller for the halo than for the inner component. A further important step forward is supplied by the finding that the only globular cluster in WLM is indeed a very old object, sharing the metallicity of the outer component field stars (Hodge *et al.* 1999). However, WLM has also a very extended gas component (see Minniti, & Zijlstra 1997) which, at least and in principle, would play against the formation of the extended component before the collapse of the galaxy had finished.

Phoenix provides an equally interesting case. Lacking gas associated to the main, optical body, this galaxy has an outer stellar component possibly (but not certainly) formed by old stars and rotated 90° with respect to the inner component (Martínez-Delgado *et al.* 1999). This fact, by itself alone, strongly indicates a possible separation of both substructures. Together with the presence of young stars in the inner component and a gas cloud at 6 arcmin away from them (Young, & Lo 1997) it makes Phoenix of mayor relevance in the study of extended components.

Centering our attention on DDO 187, we will show in this section how our data, together with information about the gas distribution, could indicate that a stellar population lacking young stars would be associated with an external, diffuse, perhaps differentiated subsystem of this galaxy. On the light of these finding, we will discuss the possible disk-halo structure on the galaxy.

6.1. The morphology of DDO 187

From surface brightness photometry, Patterson & Thuan (1996, 1998) have determined the Holmberg radius, ellipticity and position angle of DDO 187 to be $r_{26.5}^B = 50.4''$, $b/a = 0.5$ and $PA = 41^\circ$. On the other hand, for the H I component of the galaxy, Lo *et al.* (1993)

obtain $a_{\text{HI}} = 2.0'$, $(b/a)_{\text{HI}} = 0.8$, $\text{PA}_{\text{HI}} = 130^\circ$, where a_{HI} is the major axis measured to 10% of the peak flux. In other words, the gas component has a similar extension to that of the optical light integrated to the Holmberg radius, but, to the first approximation, the former shows a spherical morphology, in contrast to the likely flattened structure of the latter.

To further investigate the structure of the galaxy, we have searched the morphology of the distribution of stars to its outermost extension. We have obtained the number density of resolved stars and fitted it with ellipses. Position angles and ellipticities for different semi-major axes have been obtained with the IRAF package. Except for the inner $45''$, the ellipses show PA in the range 20° – 50° , compatible with that of the optical Holmberg radius ellipse, but with ellipticities $b/a \sim 0.7$ – 0.85 . See below for more discussion about the different components of the galaxy.

We then obtained the surface density of stars in the galaxy by counting stars in ellipses of increasing semi-major axis r . All the stars shown in the CMD of Figure 2 have been used. We have adopted $b/a = 0.85$ and $\text{PA} = 49^\circ$ for all the ellipses. These values correspond to those of the outermost ellipses, at $r > 100''$. The results are shown in Figure 7. The background level estimated from our comparison field is shown by the line in the lower right part of the figure. After subtracting this background level, we performed an exponential fit to the region $50'' \leq r \leq 120''$. The innermost part of the galaxy has been excluded to avoid completeness effects. The fit yields a scale factor $\alpha = 25.5''$, which corresponds to 310 pc at the distance of DDO 187. After scaling to the same distance, this is more than twice the result obtained by Patterson & Thuan (1996) for the surface brightness distribution, indicating that the galaxy is larger than was previously thought.

In fact, the surface brightness distribution given by Patterson, & Thuan (1996) for DDO 187 extends to $50''$, i. e. covering only the inner body of the galaxy. For this reason, roughly estimated surface brightness scales in V and I are also plotted in the right-hand vertical axis of Figure 7. The scales can be obtained making $k = 24.0$ for the case of μ_V and $k = 23.5$ for the case of μ_I and have been computed comparing the logarithmic number of stars in a region of $80 \times 80''^2$ centered on the galaxy with the integrated magnitudes of the same region. The surface brightness profile by Patterson, & Thuan (1996) is to be preferred for the inner region of the galaxy, the surface brightness scale of Figure 7 being useful for the external region. Surface magnitude of the brightest, south-west region of the galaxy, where the youngest stars are placed are $\mu_V = 22.69 \pm 0.05$ and 22.27 ± 0.05 . Errors are the zero-point errors of our photometry.

6.2. The star formation history of DDO 187

The SFH of a galaxy can be derived in detail from a deep CMD through comparison with synthetic CMDs (see Gallart *et al.* 1999). The CMD of DDO 187 is not deep enough for such a detailed analysis but it is still possible to sketch the SFH of the galaxy for old, intermediate and young ages.

The galaxy has been divided into three parts for the study of the SFH as shown in Figure 8. The inner part corresponds to the optical body of the galaxy down to the Holmberg radius, as determined by Patterson & Thuan (1996, 1998). The intermediate part matches the gas component as given by Lo *et al.* (1993), excluding the inner component. The outer part includes the rest of the galaxy out to $r = 120''$ where, according to the results given above, the galaxy seems to vanish. The resolved stars have also been plotted in Figure 8. While most of the blue and many bright red stars are in the inner component, the fainter red population extends outwards and defines the ellipticity and orientation of the outer component.

In what follows, we will discuss the derivation of the SFH for each region. Note that the different stellar populations will evolve kinematically in different ways and will not necessarily be found in the same region where they were born. So, properly speaking, what we are going to obtain is the distribution of stellar ages, with indication of stellar metallicities in each region. For simplicity, we will continue to term the combined distribution as SFH. We will look for differences in these distributions as a first indication of differences in the underlying structure and/or evolutionary history of the galaxy.

A simplified version of the method proposed by Aparicio, Gallart, & Bertelli (1997b) and used by Gallart *et al.* (1999) for Leo I has been employed to obtain the SFH of the three regions defined in DDO 187. In practice, a synthetic CMD with arbitrary, constant SFR of value ψ_p , the IMF of Kroupa *et al.* (1993), 25% of binary stars with mass ratios, q , uniformly distributed in the interval $0.6 < q < 1.0$, and a metallicity, Z , taking random values from $Z_1 = 0.0002$ to $Z_2 = 0.001$ independently of age have been used. The Z interval has been chosen considering the metallicities for H II regions given by Skillman *et al.* (1989) and by van Zee *et al.* (1997a), the value of $[\text{Fe}/\text{H}]$ given in Sec. 4, and the dispersion of colors in the red-tangle.

The resulting synthetic CMD has been then divided into four age intervals: 0–0.1 Gyr, 0.1–0.3 Gyr, 0.3–4 Gyr, and 4–15 Gyr. Following the nomenclature introduced in Aparicio *et al.* (1997b), each of these synthetic diagrams will be called a *partial model* CMD and any linear combination of them will be denoted as *global models*. Eight regions have been defined in the observed and the partial model CMDs with the criterion that they sample

different age intervals (see Gallart *et al.* 1999 and Aparicio 1999). The regions are shown in Figure 9. We will denote by N_j^o the number of stars of the observed CMD lying in region j and by N_{ji}^m the number of stars of partial model (age interval) i populating region j . The number of stars populating a given region in a global model is then given by

$$N_j^m = k \sum_i \alpha_i N_{ji}^m \quad (8)$$

and the corresponding SFR

$$\psi(t) = k \sum_i \alpha_i \psi_p \Delta_i(t), \quad (9)$$

where α_i are the linear combination coefficients, k is a scaling constant, and $\Delta_i(t) = 1$ if t is inside the interval corresponding to partial model i and $\Delta_i(t) = 0$ otherwise. The $\psi(t)$ having the best compatibility with the data can be obtained by a least-squares fitting of N_j^m to N_j^o .

In practice, several solutions can be found showing similar departures, σ , from the data. To smooth out the bias that selecting a single good solution would introduce, several are selected and averaged to obtain the best final solution. In the case of DDO 187, models showing σ values smaller than 1.5 times the σ of the best solution have been used.

The resulting $\psi(t)$ for the three regions in which DDO 187 has been divided are shown in Figure 10. The right-hand vertical scales are normalized to the area covered by each region.

The most interesting result from the SFH analysis is that the central region shows a strong increase of $\psi(t)$ for the last few 100 Myr and that the outer region shows no star formation activity, in good agreement with what is expected from the absence of gas. This will be used below for the discussion of the structure of DDO 187.

The current SFR obtained in Sec. 5 from the H_α luminosity refers to the last ~ 20 Myr. It is a factor of eight smaller than the value derived here for the last 100 Myr in the central region of the galaxy, but it is similar to the SFR averaged over the entire life-time of the galaxy. This picture favors a bursting star formation mode, with the last strong burst having taken place between 20 and 100 Myr ago. If this burst had lasted 10 Myr, its intensity would have been of $2 \times 10^{-2} M_\odot \text{ yr}^{-1}$, which is not far from the values given by Fanelli, O’Connell, & Thuan (1988) for blue compact dwarfs.

It is also interesting to note that the picture of high present-day or very recent star formation activity much higher than the average for the entire life-time of the galaxy is frequently found in galaxies classified as dIrr (NGC 6822: Gallart *et al.* 1996b,c; Pegasus: Aparicio, Gallart, & Bertelli 1997a, Gallagher *et al.* 1999; Antlia: Aparicio *et al.* 1997c).

On the other hand, galaxies like Phoenix (Martínez-Delgado *et al.* 1999) or LGS 3 (Aparicio, Gallart *et al.* 1997b), frequently considered as dSph-dIrr transition objects, show similar $\psi(t)$ histories until a few 100 Myr ago, failing only in currently producing stars at a high rate. This would also point to a bursting mode of star formation, the dSph-dIrr galaxies being in a quiescent period, and would also imply that an important bias could exist in the classification of dwarfs as bona-fide dIrrs towards objects experiencing strong star formation bursts.

The SFR averaged for different periods of time is given in Table 5 for the three regions defined in DDO 187. The first four lines give the SFR averaged for the whole life-time of the galaxy (assumed to be 15 Gyr) and for the intervals 15–1 Gyr, 1–0 Gyr, and 0.1–0 Gyr ago. Line 5 gives the current SFR derived from the H_α flux. Lines 6 to 10 give the same information as lines 1 to 5 after normalization to the area of each region.

6.3. A disk-halo structure in DDO 187?

Some of the results presented here are compatible with (but not conclusive of) a two-components, disk/halo-like structure in DDO 187. Let us assume the two-component possibility as a working hypothesis and check to what extent it could be accepted. There are three facts supporting it:

1. The high ellipticity of the inner star forming region could be due to it being a flattened, disk-like component, different from the almost spherical, low-density, outer region.
2. The gas component is spatially much more compact than the outer stellar one. This would be qualitatively compatible with a collapse that left behind the formed stars earlier.
3. The external component lacks young stars, as it would be expected in an early formed structure which was later on deprived of gas.

These three results combine both age and morphological properties, thereby giving more self-consistency to the two-component hypothesis. But all them are necessary rather than sufficient conditions. In particular, the sufficient conclusive conditions should be of the three following kinds:

1. Kinematical, and not only morphological, decoupling should exist between the inner and the outer components. Radial velocities of the stars would be necessary to determine if this is the case, but they are beyond reach of current instruments.
2. The gas should be associated with the inner, flat component, rather than showing a spherical distribution. It could be, however, that the sphericity of the gas originates in the heating produced by supernova explosions in the inner region.
3. The stellar population of the outer component should be old (older than ~ 10 Gyr), the fact that young stars lack there not being enough. With the time resolution for intermediate and old ages of the analysis presented here it is not possible to accept or reject the presence of an intermediate-age population with a high confidence level.

Summarizing, the two-component hypothesis does not seem unrealistic. But nothing can be definitely stated until more detailed data, ideally including kinematics, are available. By now, this is the case for other dwarfs for which differentiated components have been sought (Antlia, NGC 3109 and with stronger clues, WLM and Phoenix; see references above). For these, as for DDO 187, more data are needed.

7. Global properties of DDO 187

The SFR $\psi(t)$ and the new estimate of the distance obtained here have been used, together with data from other authors, to calculate the integrated properties of DDO 187 listed in Table 6. The bracketed figures refer to the bibliographic sources for each data. First the metallicity, Z , the distance to the Milky Way, d_{MW} , and the distance to the barycenter of the Local Group, d_{LG} , are given. Integrated absolute magnitudes and luminosities, referred to the Holmberg radius at $\mu_B = 26.5 \text{arcsec}^{-2}$ (which match the inner component of the former analysis) follow. M_\star is the mass in stars and stellar remnants for the whole galaxy, calculated from integration of $\psi(t)$ and assuming that 0.8 of this integral remains locked in stellar objects. M_{gas} is obtained by multiplying the H I mass by 4/3 to take into account the mass in He. M_{vt} is the virial mass obtained from the velocity dispersion of the gas. μ is the gas fraction, relative to the total mass intervening in the chemical evolution. dmf is the dark matter fraction, calculated as indicated in the table. Finally, the gas and total mass to luminosity fractions are given.

8. Conclusions

The hypothesis that dwarf star forming galaxies could have extended, primeval structures is tested for the dIrr DDO 187. Together with the SFH and the structure of DDO 187, this paper provides a new estimate of the distance and discusses the distribution of H II regions.

From the I magnitude of the tip of the red giant branch (I_{TRGB}), the distance of DDO 187 to the Milky Way is estimated to be 2.5 ± 0.2 Mpc. The distance to several neighbor galaxies and groups have been computed, showing that it is an isolated, field galaxy: DDO 187 is at 2.6 Mpc from M 94; at 2.7 Mpc from the barycenter of the Local Group, and at 3.2 Mpc from M 81; the closest dwarf galaxies to DDO 187 are GR 8, at 0.85 Mpc and DDO 190, at 1.05 Mpc.

The distance of DDO 187 to the Milky Way (2.5 Mpc) found here is quite different from the value of 7 Mpc, estimated from Cepheid light-curves by Hoessel et al. (1998). This is the third case (Pegasus, and Leo A are the other two) in which such a large disagreement is obtained between the two methods and implies that Cepheid-based distances of dwarf galaxies must be accepted cautiously. We suggest that the scarcity of Cepheids in dwarf galaxies, derived from the small amount of young stars, would not make worthwhile the effort of determining their distance with Cepheids.

DDO 187 has several H II regions. From analysis of their fluxes, it is found that the most massive star alive in the galaxy has a mass of some $30 M_{\odot}$ and that the current SFR is smaller by a factor of 3 than it was 20–100 Myr ago.

The SFH of DDO 187 has been obtained using synthetic CMDs. DDO 187 shows an overall decreasing SFR, but with high star formation activity over the last few hundred Myr in its central region. The SFR for different regions of the galaxy are summarized in Table 5. In particular, the data analyzed here are compatible with a maximum in the SFR between 20 and 100 Myr ago that could have had an intensity comparable to that of some blue compact galaxies. Interestingly, this picture of an overall decreasing SFR with a strong enhancement in the recent past is common to other dIrr galaxies. It is suggested that perhaps the dIrr morphology is only produced by the recent past SFR activity and that no large intrinsic differences exist between typical dIrrs and other dwarf galaxies showing similar intermediate- to old-age SFHs but neither H II regions nor other traces of very recent star formation activity.

Several results suggest that DDO 187 has a two-component halo/disk-like structure: (i) differentiated morphologies for the inner and outer stellar components; (ii) a gas component less extended than the outer stellar component, and (iii) an outer component lacking young

stars. The working hypothesis that a real halo/disk structure could be present is discussed. The conclusion is reached that the two-components hypothesis is not unrealistic, but that nothing can be clearly stated until more detailed data, ideally including kinematics, are available.

Finally the distance and the SFH derived in this paper have been used together with data from the literature to calculate several global parameters of DDO 187 which are given in Table 6.

This paper has been largely improved after careful reading of the manuscript by Carme Gallart and David Martínez-Delgado and after the endless, fruitful discussions maintained with them. We are also grateful to Richard Patterson and to the referee of the paper, Albert Zijlstra, for their useful comments and suggestions.

This work has been financially supported by the IAC (grants P3/94 and P90/92), by the DGES of the Kingdom of Spain (grant PB97-1438-C02-01) and by INTAS-RFBR grant 95-IN-RU-1930. Data from NED have been used.

REFERENCES

- Aparicio, A. 1994, *ApJ*, 437, L27
- Aparicio, A. 1999, in *The Stellar Content of Local Group Galaxies*. I.A.U. symp. 192, edited by P. Whitelock
- Aparicio, A., Dalcanton, J. J., Gallart, C., & Martínez-Delgado, D. 1997c, *AJ*, 114, 1447
- Aparicio, A., & Gallart, C. 1994, in *The Local Group: Comparative and Global Properties*, ESO Conference and Workshop Proceedings No. 51, edited by A. Layden, R. C. Smith, and J. Storm (ESO Garching), p. 115
- Aparicio, A., & Gallart, C. 1995, *AJ*, 110, 2105
- Aparicio, A., Gallart, C., & Bertelli, G. 1997a, *AJ*, 114, 669
- Aparicio, A., Gallart, C., & Bertelli, G. 1997b, *AJ*, 114, 680
- Aparicio, A., Gallart, C., Chiosi, C., & Bertelli, G. 1996, *ApJ*, 469, L97
- Aparicio, A., Moles, A., & García-Pelayo, J. M. 1988, *A&AS*, 74, 367
- Aparicio, A., Tikhonov, N., & Karachentsev, I. 1999, in preparation
- Bertelli, G., Bressan, A., Chiosi, C., Fagotto, F., & Nasi, E. 1994, *A&AS*, 106, 275
- Burstein, D., & Heiles, C. 1982, *AJ*, 87, 65

- Dohm-Palmer, R. C., Skillman, E. D., Gallagher, J., Tolstoy, E., Mateo, M., Dufour, R. J., Saha, A., Hoessel, J., & Chiosi, C. 1998, *AJ*, 116, 1227
- Fanelli, M. N., O’Connell, R. W., & Thuan, T. X. 1988, *ApJ*, 334, 665
- Freedman, W. L., & Madore, B. F. 1990, *ApJ*, 365, 186
- Freedman, W. L., Hughes, S. M., Madore B. F., Mould, J. R., Lee, M. G., Stetson, P., Kennicutt, R. C., Turner, A., Ferrarese, L., Ford, H., Graham, J. A., Hill, R., Hoessel, J. G., Huchra, J., Illingworth, G. D. 1994, *ApJ*, 427, 628
- Gallagher, J. S., Tolstoy, E., Dohm-Palmer, R. C., Skillman, E. D., Cole, A. A., Hoessel, J. G., Saha, A., & Mateo, M. 1998, *AJ*, 115, 1869
- Gallart, C., Freedman, W.L., Aparicio, A., Bertelli, G., & Chiosi, C. 1999, *AJ*, submitted
- Gallart, C., Aparicio, A., Bertelli, G., & Chiosi, C. 1996b, *AJ*, 112, 1950
- Gallart, C., Aparicio, A., Bertelli, G., & Chiosi, C. 1996c, *AJ*, 112, 2596
- Gallart, C., Aparicio, A., & Vilchez, J. M. 1996a, *AJ*, 112, 1928
- Hodge, P. W., Dolphin, A. E., Smith, T. R., & Mateo, M., 1999, *ApJ*, in press
- Hoessel, J. G., Abbott, M. J., Saha, A., Mossman, A. E., & Danielson, G. E. 1990, *AJ*, 100, 1151
- Hoessel, J. G., Saha, A., & Danielson, G. E. 1998, *AJ*, 116, 1679
- Hoessel, J. G., Saha, A., Krist, J., & Danielson, G. E. 1994, *AJ*, 108, 645
- Kennicutt, R. C. 1988, *ApJ*, 334, 144
- Kroupa, P., Tout, C. A., & Gilmore, G. 1993, *MNRAS*, 262, 545
- Landolt, A. U. 1992, *AJ*, 104, 340
- Lee, M. G., Freedman, W. L., & Madore, B. F. 1993, *ApJ*, 417, 553
- Lo, K. Y., Sargent, W. L. W., & Young, K. 1993, *AJ*, 106, 507
- Martínez-Delgado, D., Gallart, C., & Aparicio, A. 1999, *AJ*, in press
- Minniti, D., Zijlstra, A. A. 1996, *ApJ*, 467, L13
- Minniti, D., Zijlstra, A. A. 1997, *AJ*, 114, 147
- Minniti, D., Zijlstra, A. A., & Alonso, M. V. 1999, *AJ*, 117, 881
- Mulder, P. S., & van Driel, W. 1993, *å*, 272, 63
- Oke, J. B. 1990, *AJ*, 99, 1621
- Panagia, N. 1973, *AJ*, 78, 929

- Patterson, R. J., & Thuan, T. X. 1996, ApJS, 107, 103
- Patterson, R. J., & Thuan, T. X. 1998, ApJS, 117, 633
- Peebles, P. J. E. 1989, ApJ, 344, L53
- Saha, A., Hoessel, J. G., Krist, J., & Danielson, G. E. 1996, AJ, 111, 197
- Skillman, E. D., Kennicutt, R. C., & Hodge, P. H. 1989, ApJ, 347, 875
- Stetson, P. B. 1994, PASP, 106, 250
- Stetson, P. B., Saha, A., Ferrarese, L., *et al.* 1998, ApJ, 508, 491
- Tolstoy, E., Gallagher, J. S. Cole, A. A., Hoessel, J. G., Saha, A., Dhom-Plamer, R. C., Skillman, E. D., Mateo, M., & Hurley-Keller, D. 1998, AJ, 116, 1244
- van den Bergh, S. 1959, Pub. David Dunlap Observatory, vol. II, n. 5
- van Zee, L., Haynes, M. P., & Salzer, J. J. 1997a, AJ, 114, 2479
- van Zee, L., Maddalena, R. J., Haynes, M. P., Hogg, D. E., & Roberts, M. S. 1997b, AJ, 113, 1638
- White, S. D. M., & Rees, M. J. 1978, MNRAS, 183, 341
- Young, L. M., & Lo, K. Y. 1997, ApJ, 490, 710

Table 1. Journal of observations

Date	Object	Time (UT)	Filter	Exp. time (s)
97.07.26	DDO 187	21:50	<i>I</i>	600
97.07.26	DDO 187	22:01	<i>I</i>	600
97.07.26	DDO 187	22:12	<i>V</i>	900
97.07.26	DDO 187	22:35	<i>V</i>	900
97.07.27	DDO 187	21:46	<i>V</i>	900
97.07.27	DDO 187	22:03	<i>V</i>	900
97.07.27	DDO 187	22:18	<i>I</i>	900
97.07.27	DDO 187	22:35	<i>I</i>	900
97.07.29	DDO 187	21:04	H_{α}	900
97.07.29	DDO 187	21:19	H_{α}	300
97.07.29	DDO 187	21:25	H_{α} -cont	400
97.07.29	Field	22:20	<i>V</i>	600
97.07.29	Field	22:32	<i>V</i>	600
97.07.29	Field	22:43	<i>I</i>	500
97.07.29	Field	22:51	<i>I</i>	500

Table 2. Distances of DDO 187 to the closest galaxies and groups

Galaxy	d (Mpc)
Milky Way	2.5
Andromeda	2.9
Local Group (barycenter)	2.7
M 81	3.2
M 94 (CnVI group)	2.6
M 101	5.2
GR 8 (dIrr)	0.85
DDO 190 (dIrr)	1.05

Table 3. Cepheid and CMD-based distances of dIrr galaxies

Galaxy	d_{Cep}	n_{Cep}	Ref.	d_{CMD}	method	Ref.
DDO 187	7 ± 1.2	2	(6)	2.5 ± 0.2	TRGB	(1)
Leo A (DDO 69)	2.2 ± 0.2	4	(5)	0.69 ± 0.06	RC	(7)
				0.80 ± 0.08	TRGB	(7)
Pegasus (DDO 216)	1.75 ± 0.15	5	(4)	0.95 ± 0.05	TRGB	(2)
				0.76 ± 0.10	TRGB	(3)

References. — (1) This paper; (2) Aparicio (1994); (3) Gallagher *et al.* (1998); (4) Hoessel *et al.* (1990); (5) Hoessel *et al.* (1994); (6) Hoessel *et al.* (1998); (7) Tolstoy *et al.* (1998)

Table 4. H II regions in DDO 187

#	D (")	$F_{H\alpha}$ $10^{-15}\text{erg s}^{-1}\text{cm}^{-2}$	$L_{H\alpha}$ 10^{36}erg s^{-1}	N_L 10^{48}s^{-1}	M_\star M_\odot
1 (c)	4.7	13.79	10.32	7.53	31.5
2 (c)	3.8	4.10	3.07	2.23	22.0
3 (c)	4.1	3.16	2.37	1.73	20.5
4 (c)	6.3	0.58	0.43	0.31	14.0
5 (c)	5.6	0.41	0.30	0.22	13.5
6 (c)	5.1	0.74	0.55	0.40	14.5
7 (c)	6.7	0.82	0.61	0.44	14.8
8 (d)	39.2	21.45	16.06	11.72	...
9 (d)	27.5	6.69	5.00	3.65	...
10 (d)	18.5	0.58	0.43	0.31	...
Total	...	78.2	58.5	42.7	...

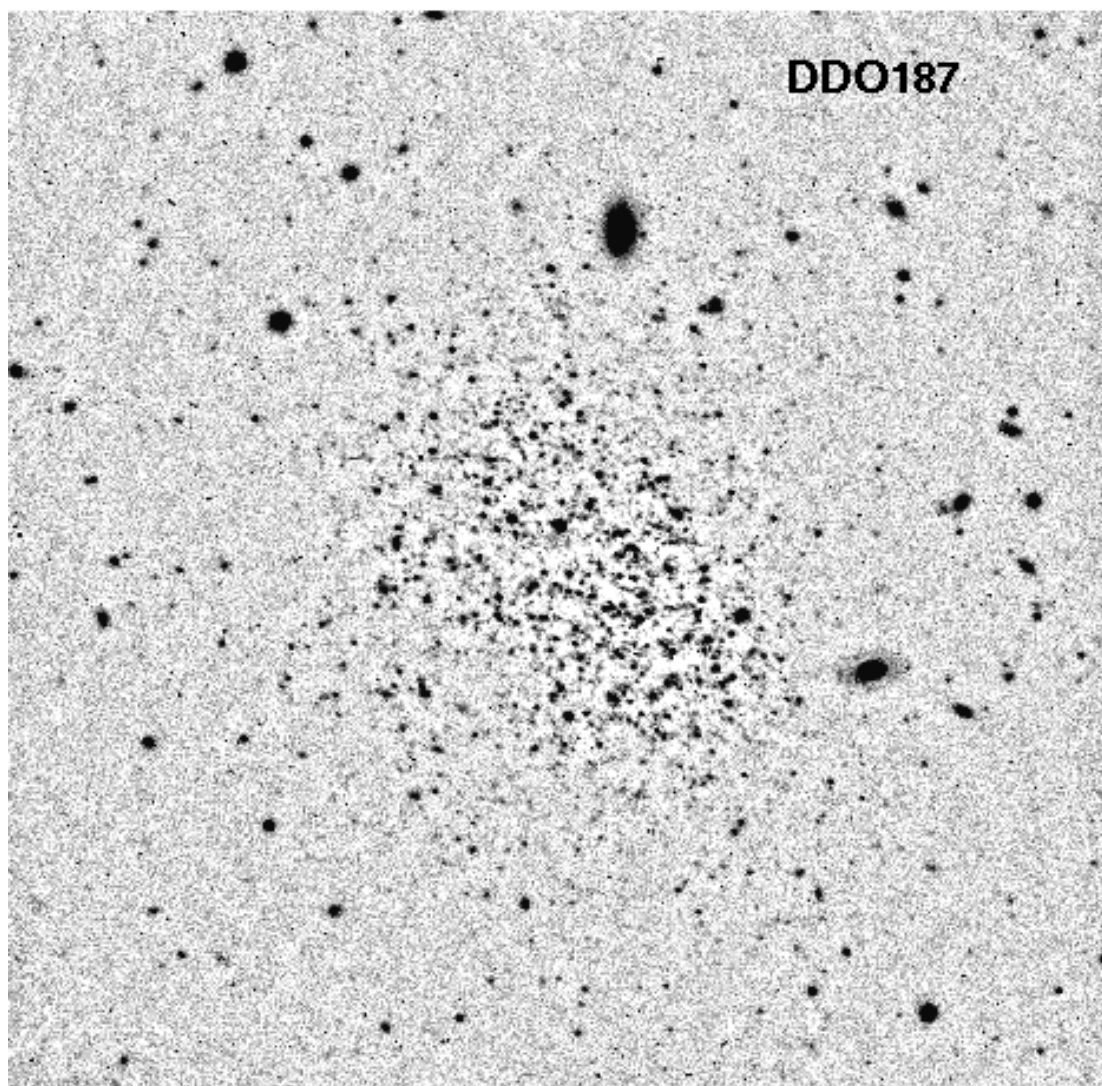
Table 5. Summary of the Star Formation History of DDO 187

	Regions:	Inner	Intermediate	Outer
$\bar{\psi}_{15-0}$	$(10^{-4}M_\odot\text{yr}^{-1})$	3.4	1.3	0.9
$\bar{\psi}_{15-1}$	$(10^{-4}M_\odot\text{yr}^{-1})$	3.1	1.3	0.9
$\bar{\psi}_{1-0}$	$(10^{-4}M_\odot\text{yr}^{-1})$	7.6	1.2	...
$\psi_{0.1-0}$	$(10^{-4}M_\odot\text{yr}^{-1})$	50	2.2	0
$\psi(0)_{\text{HII}}$	$(10^{-4}M_\odot\text{yr}^{-1})$	17.5	0	0
$\bar{\psi}_{15-0}/A$	$(10^{-9}M_\odot\text{yr}^{-1}\text{pc}^{-2})$	0.59	0.16	0.018
$\bar{\psi}_{15-1}/A$	$(10^{-9}M_\odot\text{yr}^{-1}\text{pc}^{-2})$	0.53	0.16	0.018
$\bar{\psi}_{1-0}/A$	$(10^{-9}M_\odot\text{yr}^{-1}\text{pc}^{-2})$	1.29	0.15	...
$\psi_{0.1-0}/A$	$(10^{-9}M_\odot\text{yr}^{-1}\text{pc}^{-2})$	8.41	0.28	0
$\psi(0)_{\text{HII}}$	$(10^{-4}M_\odot\text{yr}^{-1})$	2.93	0	0

Table 6. Global properties of DDO 187

$\alpha_{2000}, \delta_{2000}$		$14^{\text{h}}15^{\text{m}}56^{\text{s}}, 23^{\circ}03'13''$
l, b		$25^{\circ}.6, +70^{\circ}.5$
Z		0.0008 (6,7)
d	(Mpc)	2.5 (1)
d_{LG}	(Mpc)	2.7 (1)
$M_{V,0}$		-13.07 (5)
$M_{I,0}$		-13.28 (4)
L_B	($10^6 L_{\odot}$)	21
L_V	($10^6 L_{\odot}$)	15
L_I	($10^6 L_{\odot}$)	8.5
M_{\star}	($10^6 M_{\odot}$)	8.4 (1)
M_{gas}	($10^6 M_{\odot}$)	26 (2,3,8)
M_{vt}	($10^6 M_{\odot}$)	102 (2,3)
$\mu = M_{\text{gas}}/(M_{\star} + M_{\text{gas}})$		0.76
$dmf = 1 - (M_{\star} + M_{\text{gas}})/M_{\text{vt}}$		0.66
M_{gas}/L_V	(M_{\odot}/L_{\odot})	1.7
M_{vt}/L_V	(M_{\odot}/L_{\odot})	6.8

References. — (1) This paper; (2) Hutchmeier, & Richter (1986); (3) Lo *et al.* (1993); (4) Patterson, & Thuan (1996); (5) Prugniel, & Héraudeau (1998); (6) Skillman *et al.* (1989); (7) van Zee *et al.* (1997a); (8) van Zee *et al.* (1997b)



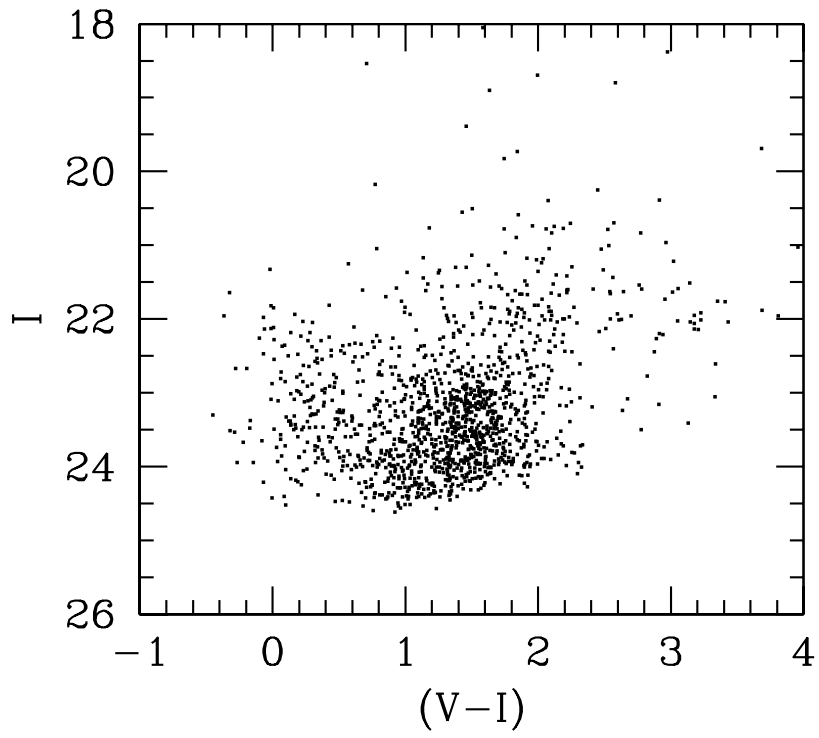


Fig. 2.— CMD of DDO 187.

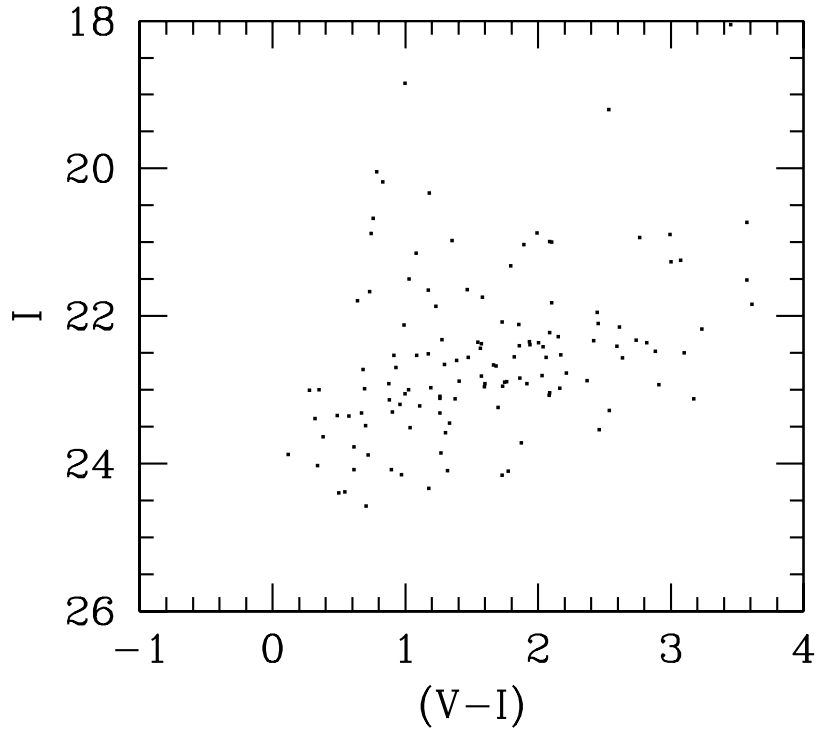


Fig. 3.— CMD of a nearby companion field mapping foreground contamination.

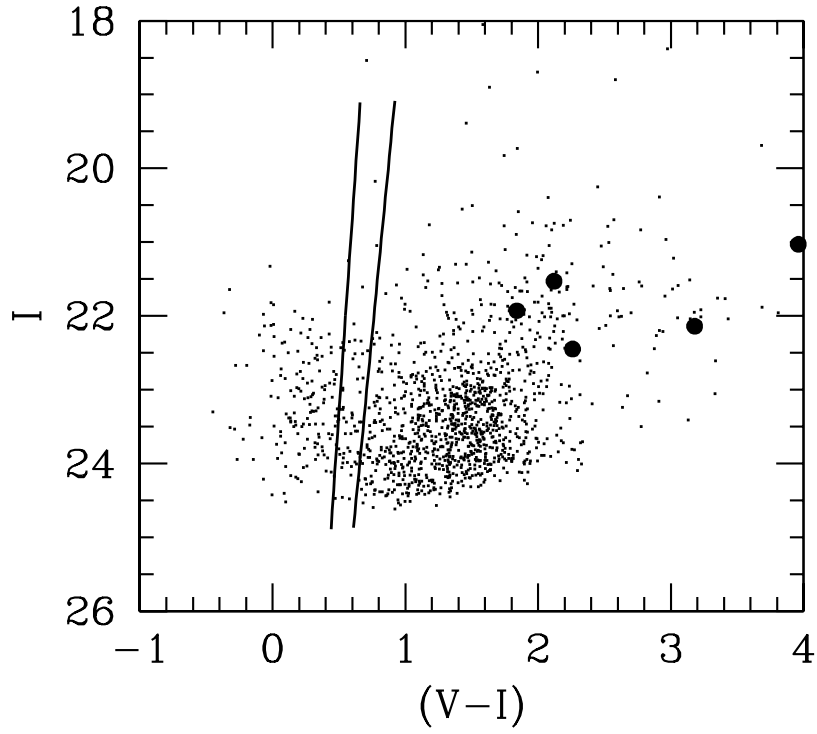
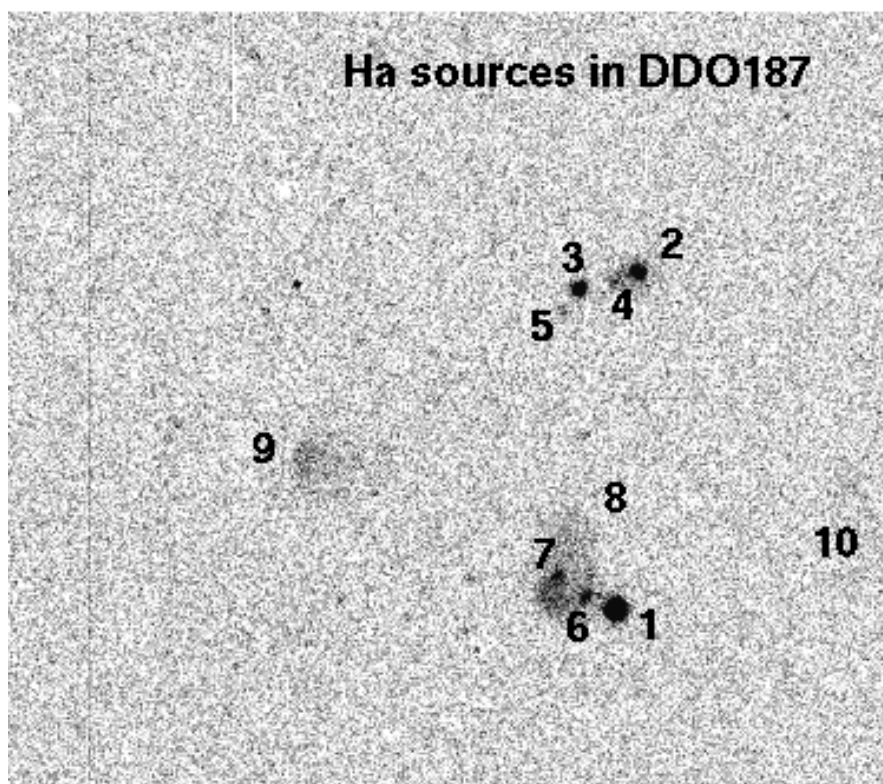


Fig. 4.— CMD of DDO187 (same as shown in Fig. 2) showing (bold dots) the Cepheid stars candidates identified by Hoessel *et al.* (1998). The Cepheids instability strip is also shown.



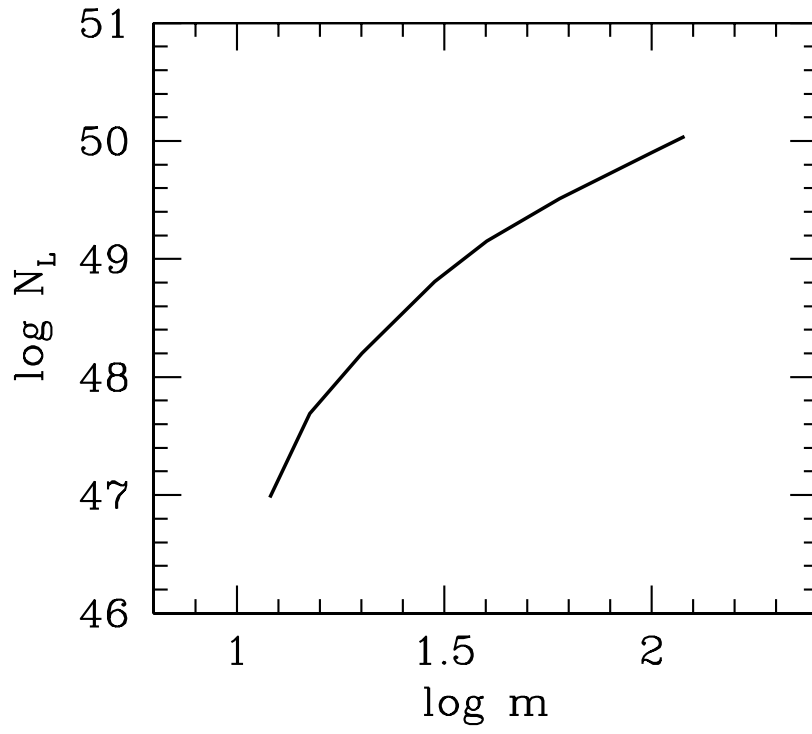


Fig. 6.— Relation between mass and Lyman photons flux for MS stars of metallicity $Z = 0.0004$.

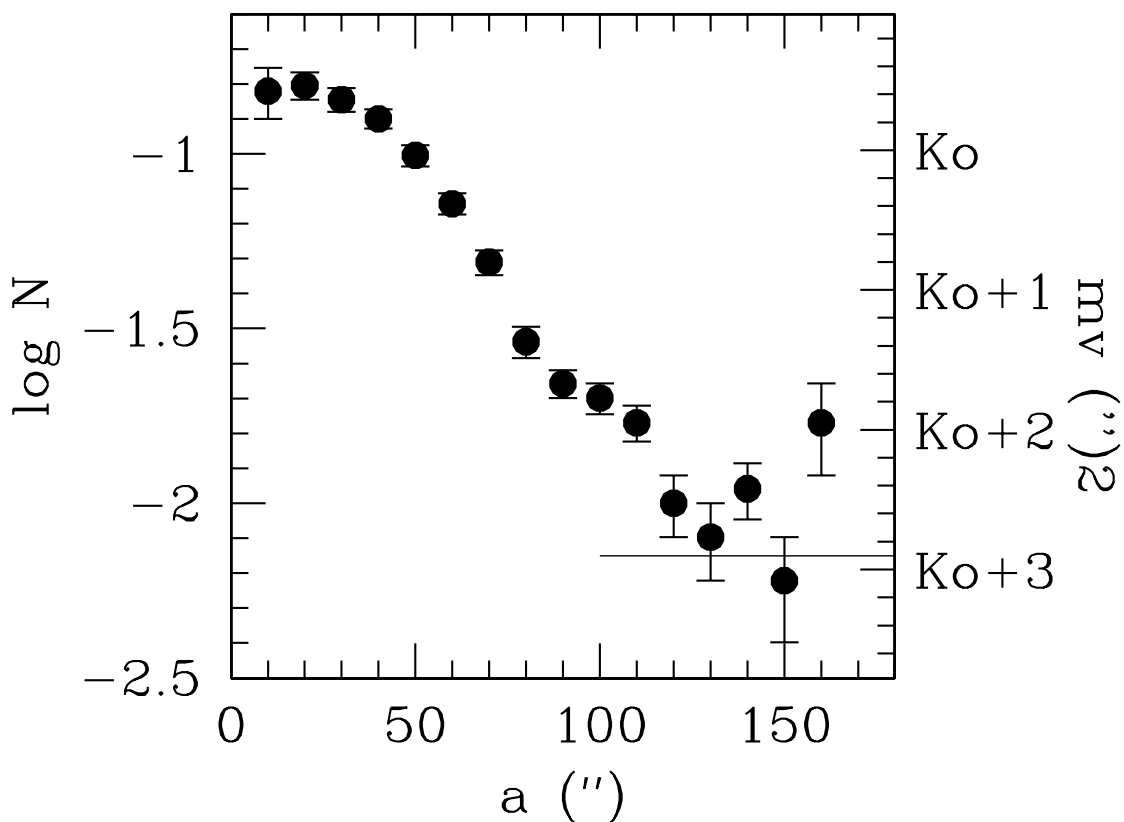


Fig. 7.— Radial distribution of resolved stars in DDO 187. The horizontal axis represents the semi-major axis distance to the galaxy center. Error bars correspond to Poisson distribution in the star counts. The line in the lower right-hand part of the figure represents the background level. The right-hand vertical axis gives rough photometrical scales for the surface brightness profiles in V and I . The scales can be obtained making $k_0 = 24.0$ for μ_V and $k_0 = 23.5$ for μ_I . See text for details.

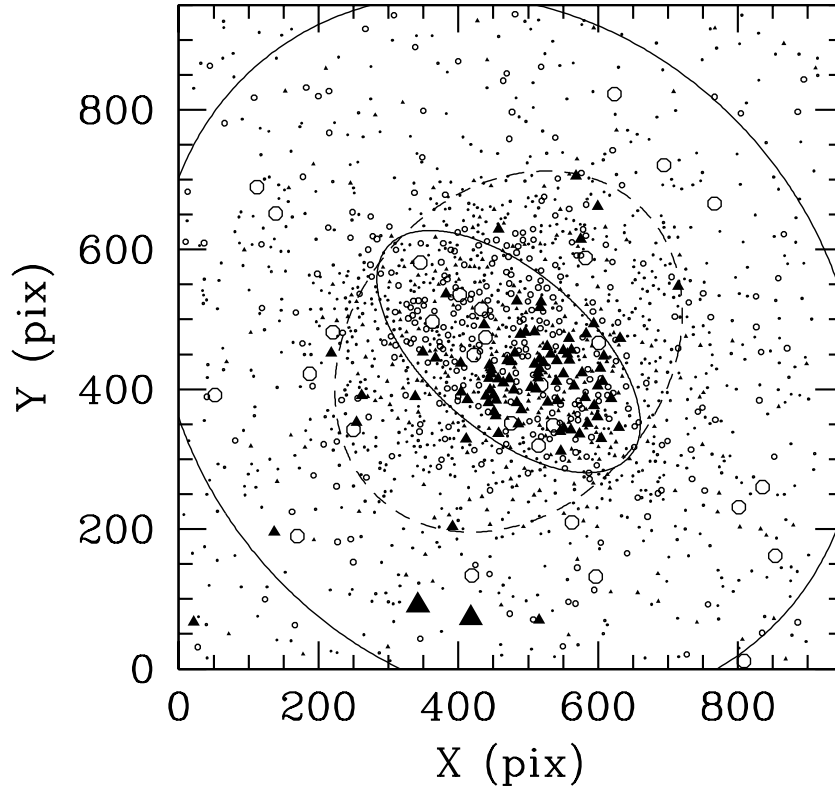


Fig. 8.— Resolved stars in DDO 187. Red stars ($(V - I) > 0.5$) are represented by open circles. Blue stars ($(V - I) \leq 0.5$) are represented by filled triangles. The three regions in which the galaxy has been divided for the morphological study are shown by the over-plotted ellipses. The inner one corresponds to the Holmberg radius (for $\mu_B \leq 26.5$), the intermediate one corresponds to the gas extension and the outermost one shows the maximum extension of the stellar component. Young stars are preferentially located in the south-west of the inner region. North is up and east is left.

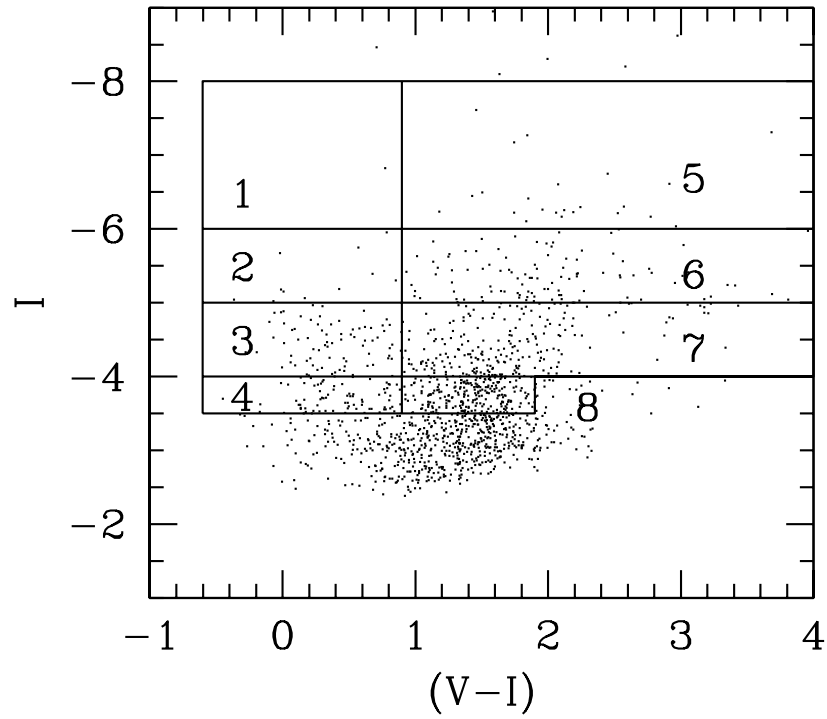


Fig. 9.— CMD of DDO187 (same as shown in Fig. 2 after correction of distance modulus $(m - M)_0 = 27.0$) showing the eight regions used to parameterize the distribution of stars of different ages.

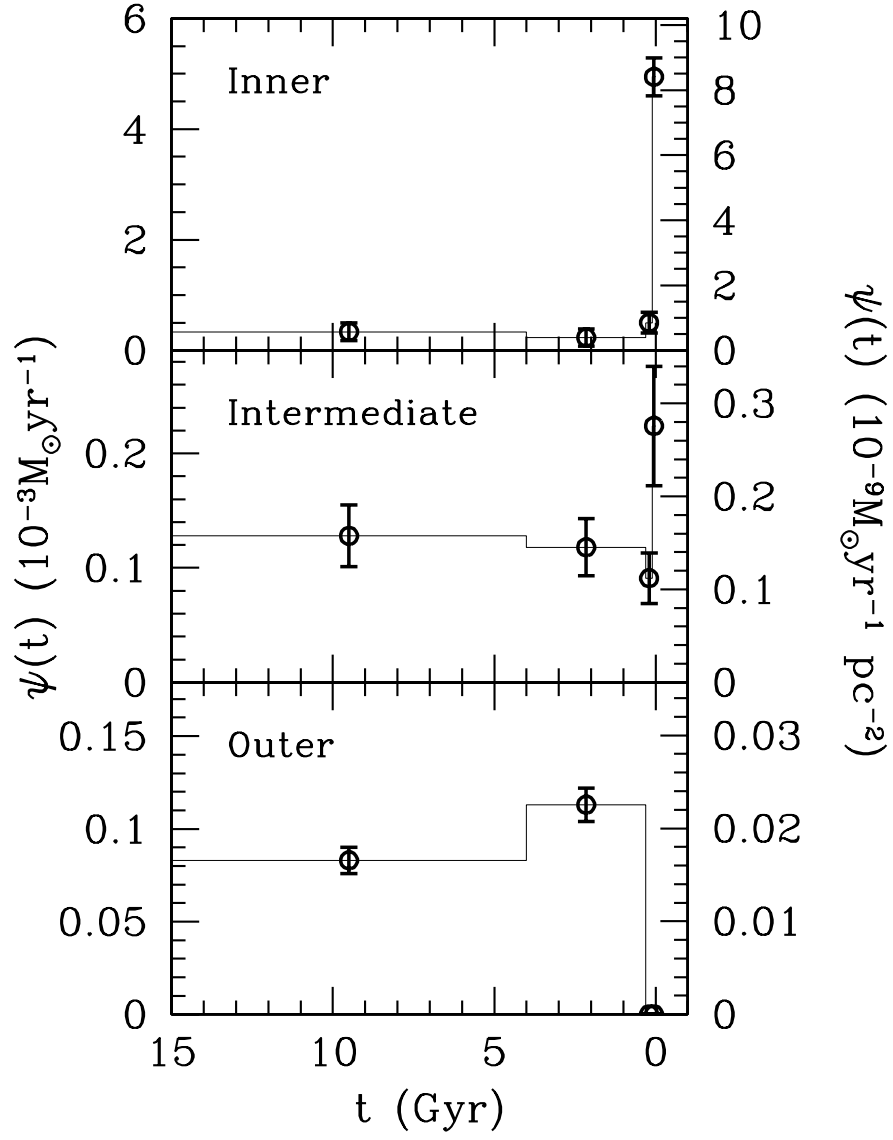


Fig. 10.— The SFR of DDO 187 as a function of time, obtained from the analysis of its CMD using synthetic CMDs.